applied sciences

MDPI

Article

Dynamic Response Analysis of Mega-Sub Isolated Structures under Multiaxial Earthquakes

Xueyuan Yan [1], Jian Liu [1], Weiyu Lin [1], Guoguan Lan [2,*] and Huimin Mao [3,*]

[1] College of Civil Engineering, Fuzhou University, Fuzhou 350116, China
[2] School of Resource Engineering, Longyan University, Longyan 364012, China
[3] School of Ecological Environment and Urban Construction, Fujian University of Technology, Fuzhou 350118, China
* Correspondence: 82013048@lyun.edu.cn (G.L.); richalmao@163.com (H.M.)

Abstract: With the use of seismic isolation techniques on mega-sub structures, several scholars have carried out research on them. However, little research has been carried out on mega-sub isolated structures under multiaxial earthquakes. There have been instances in actual engineering where the peak vertical acceleration exceeded the horizontal direction, and the vertical seismic component will also amplify the dynamic response of the structure in the horizontal direction, so in practice, it is necessary to consider the influence of the vertical component of the earthquake on the structure. To investigate the dynamic response of mega-sub isolated structures under unidirectional earthquake and coupled earthquake, this paper used numerical methods to analyze the influences of the horizontal and vertical damping ratio of the isolation layer, the horizontal and vertical frequency ratio of the main substructure, and the mass ratio of the main substructure on the acceleration and displacement of the main and substructure. The optimum parameter values are finally achieved by analytical calculations, which provide a basis for further optimization and practical design of the structure. Finally, the collision between the main and sub-structures in the mega-sub isolated structure was simulated, and the influences of the peak ground motion, main and subframe spacing, vertical seismic component, and sub-structure height on the collision force and acceleration were analyzed. It was shown that the conflict of the main and sub-structures generates instantaneous, large collision forces, which also instantaneously amplify the acceleration and base shear force response, which should be avoided in practical engineering.

Keywords: mega-sub isolated structure; numerical methods; collision forces; damping ratio; mass ratio

check for updates

Citation: Yan, X.; Liu, J.; Lin, W.; Lan, G.; Mao, H. Dynamic Response Analysis of Mega-Sub Isolated Structures under Multiaxial Earthquakes. *Appl. Sci.* **2023**, *13*, 8692. https://doi.org/10.3390/app13158692

Academic Editors: Angelo Aloisio and Dag Pasquale Pasca

Received: 8 June 2023
Revised: 19 July 2023
Accepted: 25 July 2023
Published: 27 July 2023

1. Introduction

With the development of the economy, the number of high-rise and super-high-rise buildings is increasing day by day, which poses a major challenge to the aseismic design of buildings [1]. To adapt to new needs, numerous new aseismic-resistant structural systems have emerged one after another [2–5], including mega frames. Mega frames are composed of a main frame with relatively high stiffness and sub-frames with relatively low stiffness. Mega frames have advantages such as clear force transmission, good lateral resistance, and superior aseismic performance [6,7]. To further improve the aseismic performance of mega frames, Feng and Chai et al. [8,9] proposed to relax the lateral connections between the main frame and subframes, causing relative motion between the main and subframes, thus forming a mega-sub structure.

In mega structures, the primary and substructures are separate, and it can use different connection methods between the primary and substructures, thereby achieving seismic isolation and energy dissipation for the structure. Mita et al. [10] proposed the use of traditional dampers in high-rise buildings to improve the energy dissipation capacity. Sadek et al. [11] studied the optimal parameter values of tuned mass dampers and found that the introduction of tuned mass dampers can significantly reduce the response of structures under earthquake loads. They also proposed that it is feasible to apply dampers to mega structures (forming mega sub-controlled structural systems, i.e., MSCSS). Wei et al. [12] established a two-dimensional equivalent model of MSCSS and mega frame structure and analyzed the elastic-plastic time history of the structure using observed data, and the result showed the control effect of the mega control structure is better than that of the mega frame structure. At the same time, Limazie et al. [13] studied the damping coefficient of the sub-structure, as well as the dynamic influences of the stiffness ratio and mass ratio of the main and sub-structures on the mega-controlled structure (MSCSS). The study concluded that there was a significant decrease in the dynamic response of the structure when the mass ratio was 2.38, and the stiffness ratio was 0.15–0.32. Abdulhadi et al. [14] optimized the placement of viscous dampers between the main structure and sub-structure and studied the optimal damper parameters, which further reduced the dynamic response of the structure. Shahzad et al. [15] added inverted V-shaped support to MSCSS. Built on the dynamic characteristics of the structure under seven seismic waves, it was found that this method can greatly improve the control ability of the structure response under strong earthquakes.

In addition to the use of dampers to control the dynamic response of the mega sub-structure, it also can use isolation sub-structure to control the dynamic response of the structure, and this method can avoid the structure from the P-delta influence caused by large overturning moments and high center of gravity [16,17]. Lan Shu, et al. [18,19] proposed setting laminated rubber bearings between the main and sub-structures and conducted experimental research, and the results showed that this method could significantly reduce the dynamic response of the structure. However, it is necessary to optimize the number and location of isolation sub-structures. Subsequently, Li et al. [20] studied the dynamic characteristics of the structure under different parameters, considered the number and location of sub-structures, and proposed a parameter optimization scheme with the base shear force as the optimization objective. They found that increasing the number of isolation sub-structures can improve the control performance of the structure. Further, Tan et al. [21] established the equations of motion of the mega-sub isolated structure and investigated the principle of isolation of the structure by using a simplified concentrated mass model, and it was found that the performance of both the seismically isolated and non-seismically isolated sub-structures in the mega sub isolated structure was better than that of the aseismic structure through experimental studies. Anajafi et al. [22] proposed the method of partial mass isolation, which can provide multiple vibration suppressors for buildings by isolating different mass parts of different floors, and this method effectively combines traditionally tuned dampers and seismic isolation techniques, resulting in a better aseismic performance of the structure.

On the other hand, the action of the earthquake load on the structure can be decomposed into two horizontal components and one vertical component, and there are few studies related to the current mega sub-isolated structure under multiaxial earthquake action. It is not enough to consider only horizontal seismic motion for some buildings with complex and important structures [23], there are multiple instances in practical engineering where the peak vertical acceleration is greater than the horizontal direction [24–26]. In addition, Furukawa et al. [27] conducted vertical shaking table tests on an isolated structure. The results indicated that vertical vibration significantly amplifies the vertical acceleration response of the structure. Guzman et al. [28] designed a bearing and applied to a steel frame structure to form a seismic isolated structure. It conducted shake table tests on it under coupled horizontal and vertical earthquake excitation. The results showed that the horizontal acceleration response values of the seismically isolated structure under coupled earthquake excitation were significantly amplified. Meanwhile, Yan et al. [29] conducted a shaking table test study on the mega-sub 3D seismic isolated structure and found that the 3D seismic isolation bearing could ensure the vertical isolation and tuned damping effect without making the seismic isolation layer have excessive vertical displacement. De Domenico et al. [30] researched Unbonded fiber-reinforced elastomeric isolators (UFREIs), and it was found the isotopically coupled biaxial hysteretic behavior of UFREIs from the test. The vertical earthquake load can influence the mechanical properties of the bearing in the horizontal direction. Considering the actual stress state of the bearing when the earthquake occurs, an efficient nonlinear phenomenological model was proposed to simulate the mechanical behavior of seismic isolation bearings.

The design of the structure needs to be considered in many aspects, such as the cumulative influence of earthquake swarm (which refers to the occurrence of consecutive earthquakes in the same area within a short time) [31], which will cause the structure to be subjected to earthquake loads several times within a short time, thus increasing the earthquake response of the structure. Moreover, because a certain relative displacement is generated between the sub-structure and the main structure during the earthquake action when the actual earthquake exceeds the seismic intensity, the relative displacement may exceed the width of the seismic isolation joints and thus lead to the collision between the sub-structure and the main structure. In order to avoid large losses due to collision, it is necessary to research and analyze the collision problem of the main and sub-structure. This article considers the impact of vertical earthquakes, conducts dynamic response analysis on the mega sub-isolated structure, explores the impact of various parameter changes on the seismic reduction effect of the structure, and identifies the optimal parameter values for better design and optimization of the structure.

2. Mega-Sub Isolation Structural Model

The model has 25 floors, with a total plan size of 30 m $\times$ 48 m and a total height of 97.5 m, and each floor of the sub-frame is 3.9 m. The mega-beams are made of H-beams, with a total height of 3.9 m and a width of 6 m; the mega-columns are arranged at the four corners of the building plan and combined with the mega-beams to form a three-floor main frame structure. There are three sub-structures between the foundation and the mega-beam and between the mega-beam and the mega-beam, named subframes 1, 2, and 3, respectively, from the bottom up. The isolation joints between the main frame and the sub-structure are 400 mm wide. In the mega-sub isolated structure, the first sub-frames are only solidly connected to the foundation and have no connection with the surroundings and top of the main frame. Furthermore, the maximum displacement of the ground floor subframe under rare earthquakes is empirically calculated to be less than 400 mm, so the influence of the sub-structure is ignored in the following analysis, as shown in Figure 1. A seismic isolation layer formed by seismic isolation bearings is provided between the main and sub-structures.

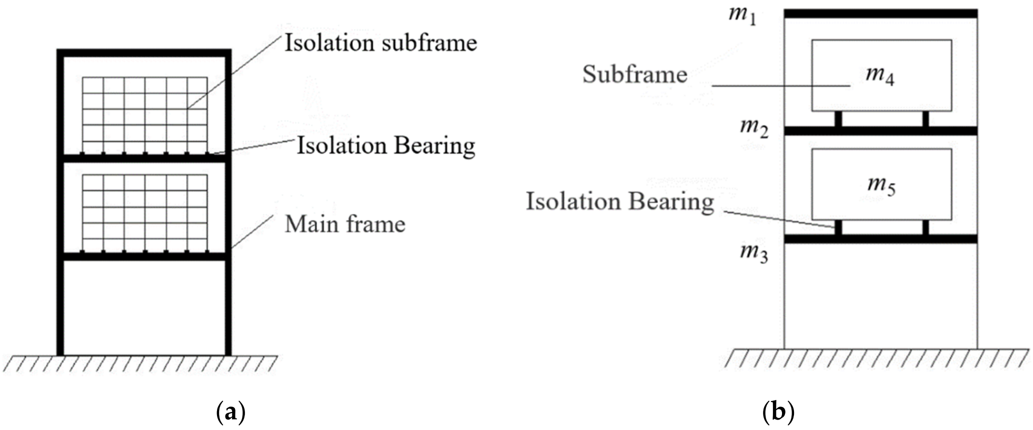

Figure 1. Simplified process for calculating the model: (**a**) Mega-sub isolation structural model; (**b**) Computational model.

In this paper, using the model shown in Figure 1 [32,33], the vibration isolation substructure is simplified to a single mass point. In the calculation example: the main frame with three layers, as shown in Figure 1, m_1 = 17.44 × 10^5 kg, m_2 = 17.96 × 10^5 kg, m_3 = 19.24 × 10^5 kg; in the substructure, m_4 = m_5 = 19.24 × 10^5 kg. The horizontal stiffness of the main frame from bottom to top is k_{1x} = 2.3 × 10^8 N/m, k_{2x} = 2.8 × 10^8 N/m, k_{3x} = 3 × 10^8 N/m; the horizontal stiffness of isolation layer is provided by the horizontal stiffness of bearing, in which the horizontal stiffness of substructure isolation layer is: k_{4x} = 5.3 × 10^7 N/m, k_{5x} = 4.6 × 10^7 N/m. The vertical stiffness of the main frame is taken from the top to the bottom floor as, k_{1z} = 8.72 × 10^9 N/m, k_{2z} = 10.72 × 10^9 N/m, k_{3z} = 11.52×10^9 N/m. The vertical stiffness of the sub-structure seismic isolation layer is, respectively, k_{4z} = 2.31 × 10^9 N/m and k_{5z} = 1.96 × 10^9 N/m. The damping ratio of the main frame was taken as 0.05. The peak displacement dynamic response was used as an indicator to study the variation law. The parameters of the seismically isolated structure in the horizontal direction are first investigated, followed by the analysis of the parameters in the vertical direction. Sheng et al. [34] carried out an earthquake dynamic time course analysis and found that: the earthquake response of main and sub-structures under the action of different seismic waves are different, and the dynamic response of the structure is largest under El Centro seismic wave. Meanwhile, Xin et al. [35] summarized the main earthquake response time analysis methods and their characteristics. According to the above-simplified model, in order to better parameterize the mass, stiffness, and damping, the Newmark-β time integration method was finally used to study the influences of El Centro seismic wave, parameters, ground shaking excitation direction and other relevant parameters on the dynamic response of the main and substructure in conjunction with the research content of this paper. At the same time, the horizontal and vertical parameters were studied and analyzed using MATLAB programming software (version 7.0) with good data processing and graphical presentation capabilities to study better the collision of the main and substructure of the mega-sub isolated structure. The collision simulation was carried out using ETABS software (version 2013) and linear elastic collision units. The relevant research content is shown in Table 1.

Table 1. Study content.

	Seismic Waves	Research Content	Study Parameters	Direction of Ground Shaking Excitation
Parametric analysis in the horizontal direction	El Centro wave	Displacement and acceleration peak response of the top layer of the main frame	Damping ratio, mass ratio, frequency ratio	X
Vertical parameter analysis	Vert-El Centro wave	Subframe vertical acceleration, seismic isolation layer displacement	Damping ratio, frequency ratio	X + Z
Mainframe and sub-frame collision	El Centro wave	Collision forces, base shear, acceleration	Ground shaking, main-substructure spacing, Vertical earthquake, subframe height, acceleration (0.3 g, 0.4 g, 0.5 g, 0.6 g, 0.7 g)	X + Z

3. Analysis of the Influence of Horizontal Parameters of the Mega-Sub Isolated Structure

3.1. Analysis of the Influence of the Horizontal Damping Ratio of the Seismic Isolation Layer

Inputting an X-direction El Centro seismic wave with the peak value of ground motion acceleration of 0.15 g, with the change of the damping ratio ξ of the isolation layer (0.05–0.5), the variation law of the acceleration of the second isolation sub-frame and the displacement response of the isolation layer is shown in Figure 2.

It can be seen from Figure 2 that, for acceleration, when the damping ratio ξ of the isolation layer is less than 0.2, the acceleration response of the isolation sub-frame decreases sharply with the increase of the damping ratio; when the damping ratio ξ is (0.2–0.3) [36–39], the peak response of acceleration decreases slowly, at which time the damping rate of the sub-frame reaches more than 50% and the damping effect is relatively better. When the damping ratio continues to increase, it causes the shear deformation of the seismic isolation layer to become relatively smaller, the energy dissipation decreases, and the acceleration response increases instead. As the damping ratio increases, the displacement becomes smaller and nearly linear.

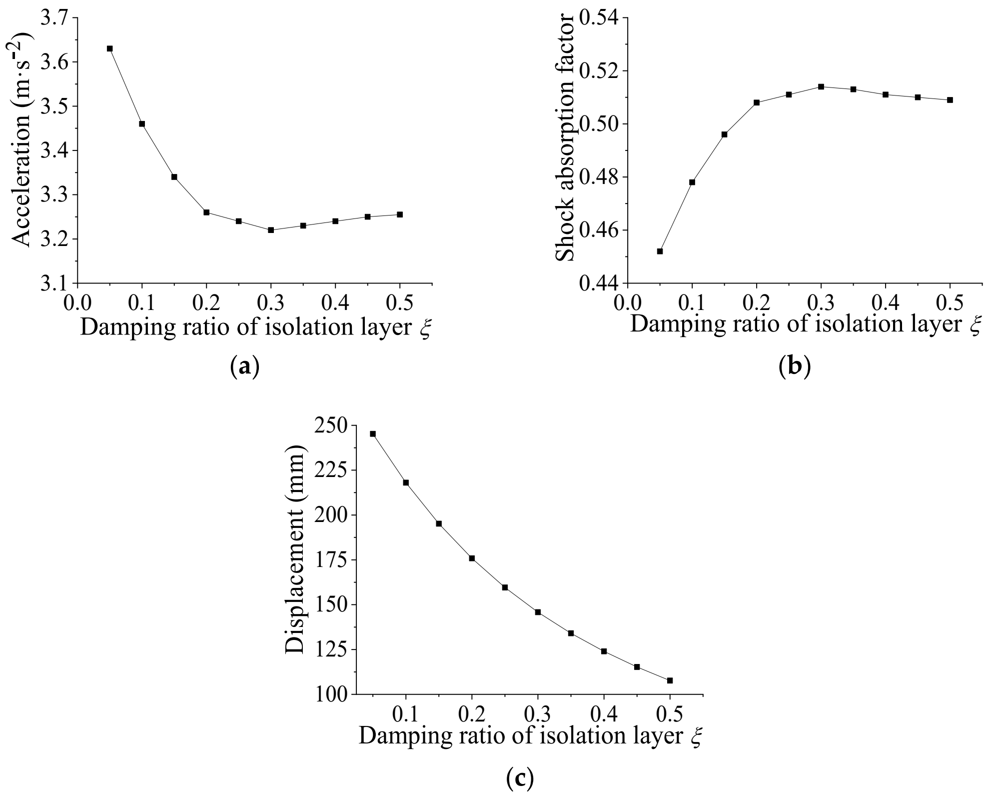

Figure 2. Variation of sub-frame dynamic response: (**a**) Variation in sub-frame acceleration; (**b**) Acceleration absorption factor change; (**c**) Variation in seismic isolator displacement.

Through the analysis and study of the damping ratio of the isolation layer in this section, we know that: for the seismic isolation subframe, the best damping effect is achieved when the damping ratio is around 0.3; in the seismic isolation design of the mega-sub structure, considering the comfort and the economy of the design of the seismic isolation bearing, it is recommended to design the damping ratio of the seismic isolation bearing at around 0.3, which is a better damping effect and more economical and reasonable.

3.2. Analysis of the Influence of the Horizontal Mass Ratio of the Seismic Isolation Layer

Each vibration isolation subframe in the mega-sub isolation structural system is a normal frame structure and a large FM (Frequency Modulation) mass block. This structure has an FM damping effect and a basic seismic isolation function. Under earthquake action, the main frame is subjected to its inertial forces and the inertial forces from the individual damped sub-frames. The inertia forces of the sub-frames are transferred to the main frame through the isolation device and partially offset by the inertia forces of the main frame. As a result, the dynamic response of the main frame is reduced.

In the ordinary FM mass damping system, the mass block is attached to it, and its weight is generally about 1% to 5% of the total weight of the structure, and the number of arrangements is small. In the mega-sub isolated structure system, the weight of each sub-frame can reach 60% to 80% of the total weight of the structure, which means that the weight of the mass block can reach more than 200% of the main structure, and more vibration isolation subframes can be arranged. Therefore, the research on the dynamic response of a mega-frame structure with varying masses of isolated subframes can help to optimize the design of mega-isolated structures.

3.2.1. Mass Ratio Influence on Main Frame Response

In the following, the change of the mass ratio of the primary and secondary frame is realized by changing the mass of the isolation subframe, and the research and analysis are carried out. The mass ratio ω is defined as (ω = total mass of the isolation sub-frame/total mass of the mega-frame), and the value of the mass ratio ω is the range is (0.1–4.5), and the damping ratio of the isolation layer is 0.3.

Inputting an X-direction El Centro seismic wave whose seismic acceleration peak value is 0.15 g, the displacement and acceleration response peak values of the top layer of the main frame vary with the mass ratio as shown in Figure 3 below.

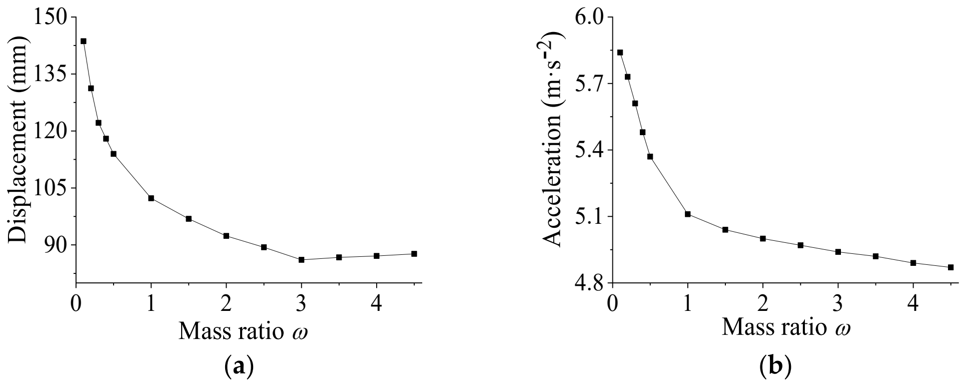

Figure 3. Variation of main frame dynamic response: (**a**) Mass ratio influence on main frame displacement; (**b**) Mass ratio influence on main frame absolute acceleration.

From the dynamic response curve of the main frame, it can be seen that the peak displacement and acceleration tend to decrease overall with increasing mass ratio ω, with the following pattern.

(1) For the displacement response of the main frame, as the mass ratio ω is less than 1.0, the displacement of the top floor of the main frame decreases faster as the mass ratio increases, i.e., the mass of the isolated substructure increases; when the mass ratio continues to increase by more than 1.5, the peak displacement response trend continues to decrease until it flattens out.

(2) For the acceleration response, when the mass ratio ω is between (0.1 and 1.0), the acceleration decreases relatively quickly, and the acceleration response is more sensitive to the change in mass ratio; when the mass ratio continues to increase, the acceleration decreases very slowly and tends to level off, and the damping effect is better at this time.

From the data, when the mass ratio ω is greater than 2.5, the main frame displacement and acceleration response peaks are smaller. The vibration-damping effect is relatively better, and increasing the mass ratio has little influence on the structural response. Considering the actual situation of the project, it is recommended to set the mass ratio between 2.5 and 4.0; at this time, the mass of the substructure reaches 71.4% to 80% of the total weight of the building.

3.2.2. Influence of Mass Ratio on Subframe Response

The response variation curve of the second isolation sub-frame is shown in Figure 4 below. It can be seen from the acceleration change curve that when the mass ratio is less than 1.0, the acceleration response decreases rapidly with the increase of the mass ratio. When the mass ratio continues to increase, the acceleration response of the sub-frame decreases slowly, reaches the minimum value at 2.0, and then increases slightly, eventually leveling off. The displacement of the isolation layer increases rapidly and then decreases with the mass ratio, and finally tends to be gentle. When the mass ratio is 1.5, the displacement reaches the maximum. When the mass ratio exceeds 3.0, the displacement response tends to be flat.

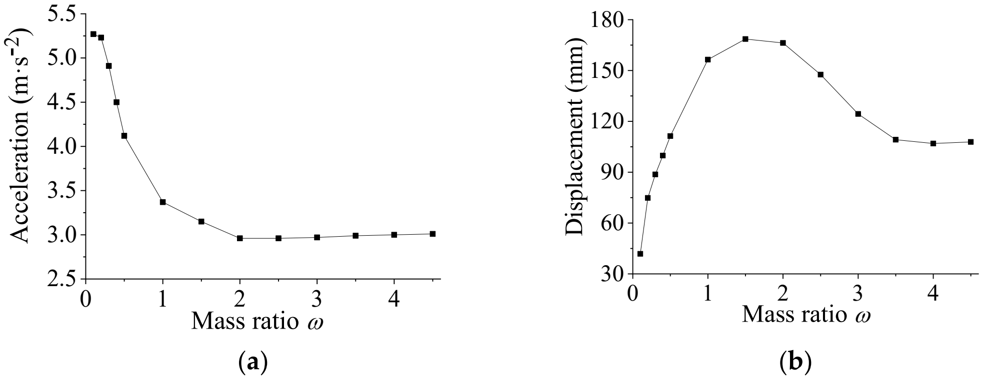

Figure 4. Variation of subframe dynamic response: (**a**) Acceleration change of the sub-frame; (**b**) Change in the displacement of the seismic isolation layer.

When the mass ratio ω is around 3.0, the second seismically isolated sub-frame isolation layer's displacement and acceleration response values are smaller, and the damping effect is better at this point. In conjunction with the analysis of the main frame above in this section, it is recommended that the mass ratio ω be set at around 3.0 for the design of a mega frame seismic isolated structure, where the total weight of the sub-frame accounts for around 75% of the total weight of the building.

3.3. Analysis of the Influence of the Horizontal Frequency of the Seismic Isolation Layer

The mega frame isolated structure has set isolation bearings between the subframe and the main frame. On the one hand, the earthquake energy is dissipated by the damping effect of the isolation bearings to achieve the purpose of energy consumption. On the other hand, the isolation bearings prolong the natural vibration period of the subframe and form a multi-frequency-modulated mass vibration reduction system. The isolation subframe plays the role of frequency modulation, thus changing the natural vibration period of the whole structure.

In this section, the change in frequency ratio of the main and sub-frame is achieved by changing the stiffness of the seismic isolation layer of the sub-frame. The self-oscillation circle frequency of the main and subframe is achieved by the following equation, which defines the frequency ratio $f = \omega_s/\omega_q$, (ω_s is the self-oscillation circle frequency of the vibration isolation sub-frame and ω_q is the first order self-oscillation frequency of the main frame). Since the stiffness of the vibration isolation layer cannot be taken too high to ensure the damping effect of the subframe, the frequency ratio f is set in the range (0.1 to 1.2).

$$\omega_s = \sqrt{(k_s/m_s)} \tag{1}$$

$$\left|K_q - \omega_q^2 M_q\right| = 0 \tag{2}$$

where ω_s is the self-oscillation frequency of the isolated subframe, k_s and m_s are the stiffness of the isolation layer and the mass of the sub-structure, respectively, ω_q is the self-oscillation frequency of the main frame (the first order self-oscillation frequency is taken in this example), K_q and M_q are the stiffness matrix and mass matrix of the main frame, respectively.

3.3.1. Influence of Frequency Ratio on Main Frame Response

The variation curves of the peak displacement and acceleration dynamic response of the top floor of the main frame with the frequency ratio f are shown in Figure 5. It can be seen that the displacement and acceleration peaks change with the frequency ratio in a relatively consistent manner, with the peak response decreasing first and then increasing, with the displacement and acceleration response peaks reaching a minimum when the frequency ratio f is around 0.6, which has a very good Isolation effect at this time.

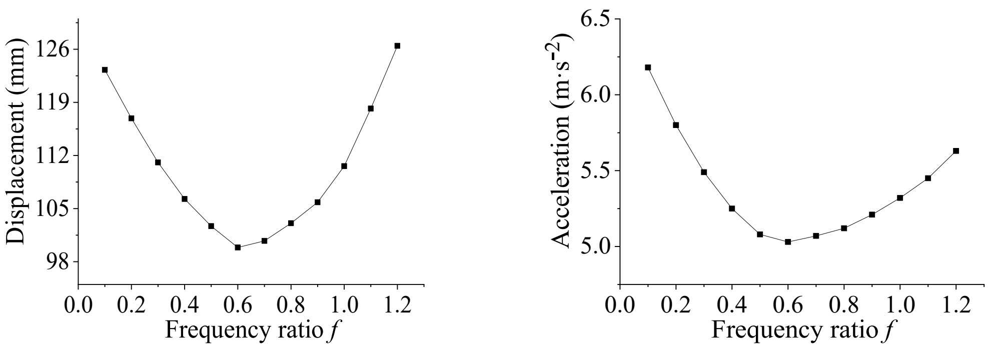

(**a**) (**b**)

Figure 5. Variation of main frame dynamic response: (**a**) Displacement change curve of the top floor of the main frame; (**b**) Absolute acceleration change curve of the top layer of the main frame.

3.3.2. Influence of Frequency Ratio on Sub-Structure Response

As shown in Figure 6, the peak acceleration response curve of the isolated subframe is similar to that of the main frame, which is in the shape of a quadratic parabola, and the best isolation influence is achieved when the frequency ratio f is greater than 0.6. The displacement of the seismic isolation layer decreases as the frequency ratio increases. When the frequency ratio f is greater than 0.6, the decrease gradually decreases and tends to level off.

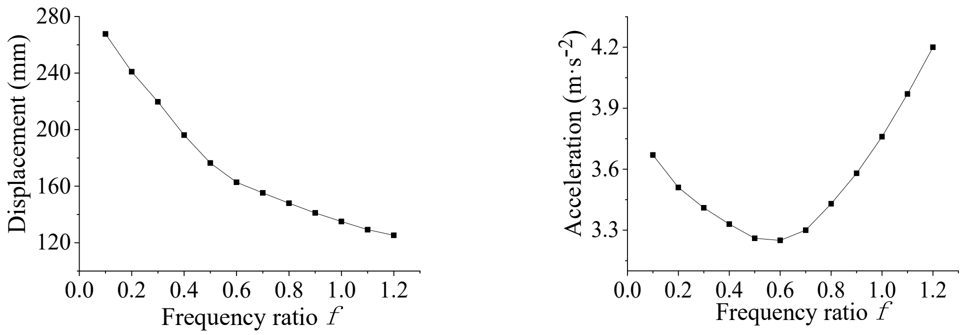

(**a**) (**b**)

Figure 6. Variation of subframe dynamic response: (**a**) Acceleration change curve of the top layer of the sub-frame; (**b**) Displacement variation curve of the seismic isolation layer.

According to the analysis in this section, the response laws of the main frame and the subframe are similar when the frequency ratio changes. When the frequency ratio f is kept at about 0.6, the main frame's displacement and acceleration peak and the isolation subframe's acceleration peak are small, which has a good damping effect; The displacement of the isolation layer is also small. Therefore, it is recommended to set the frequency ratio at about 0.6 in the actual design.

4. Analysis of the Influence of the Vertical Parameters of the Mega-Sub Isolated Structure

4.1. Analysis of the Influence of the Vertical Damping Ratio of the Seismic Isolation Layer

The vertical dynamic analysis was performed on the seismically isolated structure. The input ground shaking acceleration peaks are the Vert-El Centro seismic wave in the X and Z directions of 0.31 g, with the acceleration peaks scaled by 1:0.65. The vertical damping ratios were taken to be the same for both seismic isolators and ranged from (0.05 to 0.5).

Influence of Vertical Damping Ratio on the Response of Seismically Isolated Subframes

The variation of vertical acceleration and seismic isolation layer displacement with a vertical damping ratio of the sub-frame under the vertical earthquake action is shown in Figure 7.

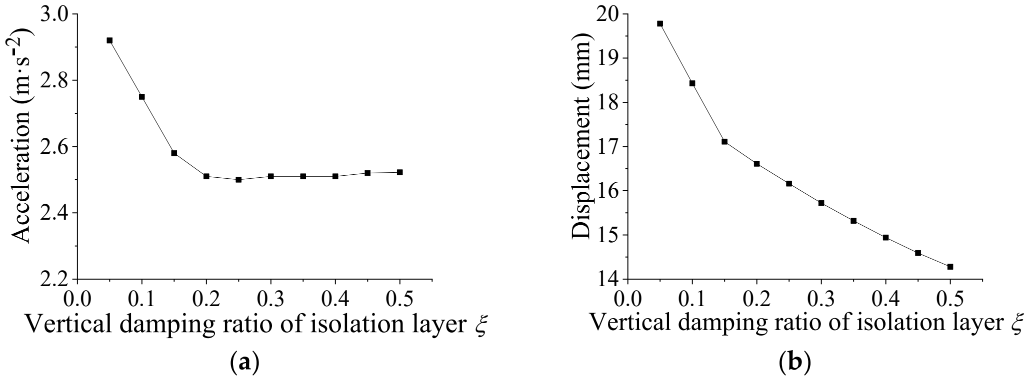

Figure 7. Dynamic variation curve of the vibration isolation substructure: (**a**) Sub-frame acceleration variation curves; (**b**) Vertical displacement curve of the isolation layer.

As seen from the above graph, after the vertical damping ratio is greater than 0.2, the subframe acceleration remains constant, and the damping ratio is no longer a factor affecting the dynamic response. For the vertical displacement of the seismic isolation layer, its value decreases as the damping ratio increases, and the change becomes smaller when the damping ratio is greater than 0.15.

For the seismic isolation subframe, the vertical damping ratio has a certain influence on its response, and the control effect does not change much when the vertical damping ratio is greater than 0.2. Therefore, it is recommended that the vertical damping ratio of the seismic isolation layer be adjusted to approximately 0.2 in the design.

4.2. Analysis of the Influence of Vertical Frequency Ratio

In the following section, the vertical stiffness of the seismic isolation layer is varied to change the vertical self-oscillation frequency of the isolated substructure. The dynamic response of the main and substructure is obtained as a function of the vertical self-oscillation frequency ratio η (η = vertical self-oscillation frequency of the isolated substructure/first-order vertical frequency of the main frame) where the self-oscillation frequency of the isolated substructure is calculated according to Equation (3).

$$\omega_z = \sqrt{(K_{s,z}/m_s)} \tag{3}$$

In the above equation, ω_z is the vertical self-oscillation frequency of the isolated substructure, $K_{s,z}$ is the vertical stiffness of the isolated substructure, taken as the sum of the vertical stiffnesses of the isolated bearings, and m_s is the substructure mass.

4.2.1. Influence of Vertical Frequency Ratio on Response of Main Frame

From the above curves, the vertical displacement and acceleration of the top floor of the mainframe are the same under the vertical earthquake action. The reason is that as the vertical frequency ratio increases, the subframe tends to consolidate and lose its tuned damping effect, increasing the dynamic response. The response is lowest when the frequency ratio between the main and sub-frame is around 1.2. However, the mainframe's peak vertical displacement and acceleration of the main frame do not change much after the frequency ratio η is greater than 1.0.

Figure 8 shows the curves of displacement and acceleration dynamic response of the top floor of the main frame with the vertical frequency ratio of the main and substructure.

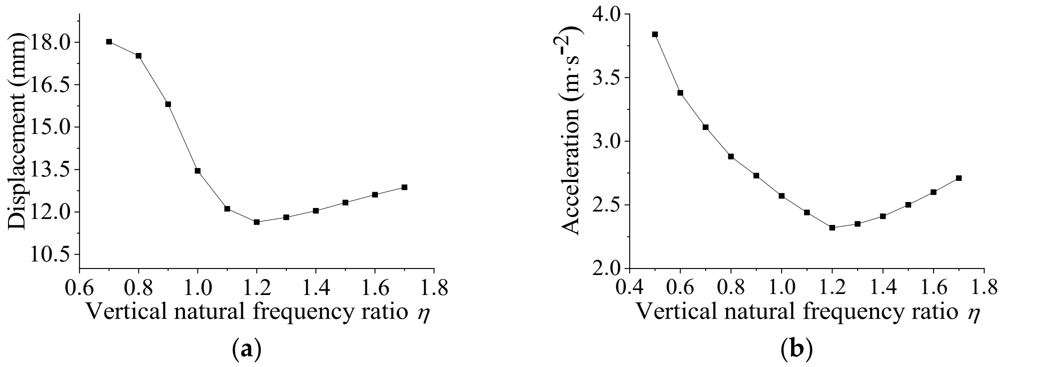

Figure 8. Vertical dynamic variation curve at the top of the mainframe: (**a**) Vertical displacement curve of main frame; (**b**) Vertical acceleration curve of the mainframe.

4.2.2. Influence of Vertical Frequency on the Response of the Seismically Isolated Subframe

Under the vertical ground motion, the isolation sub-frame acceleration and the isolation layer's vertical displacement response vary with the frequency ratio, as shown in Figure 9.

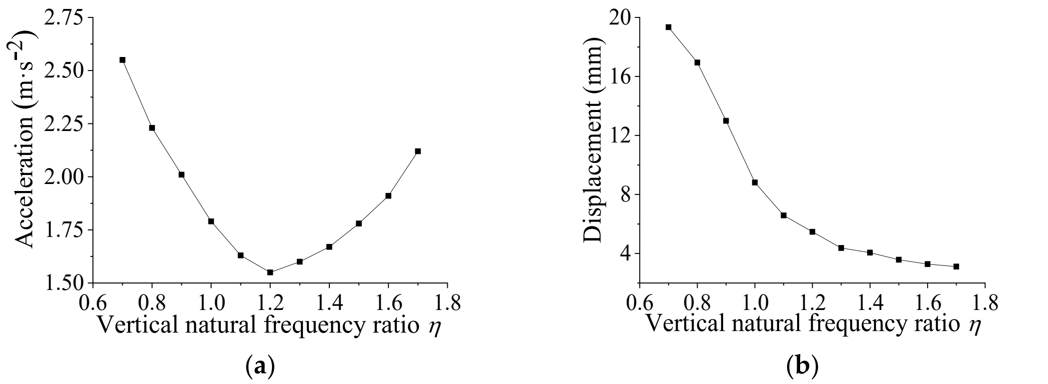

Figure 9. Subframe dynamics variation curve: (**a**) Vertical acceleration curve of sub−frame; (**b**) Vertical displacement curve of isolation layer isolation layer.

From the above curve, the vertical acceleration of the sub−frame first decreases and then increases with the frequency ratio η and reaches the minimum value at 1.2; for the vertical displacement of the isolation layer, the vertical relative displacement response value increases with the frequency of the increase of the ratio have always shown a decreasing trend. When the frequency ratio η is greater than about 1.1, the decrease in the response value tends to be gentle.

5. Parametric Analysis of Main and Sub−Frame Collisions

5.1. Influence of Collision on Structural Response

The collision between the main and sub−frame was achieved by increasing the seismic wave acceleration to analyze the dynamic response under the collision of the main and sub−frame. Three different seismic waves, the El Centro wave, Taft wave, and artificial wave, were input in the X direction of the structure, and the peak acceleration was adjusted to 0.4 g. The collision stiffness in the line Elastic collision unit was set to 5.0×10^7 kN/m, used to simulate rigid collisions between the main and sub−frames.

To facilitate the analysis of collision results, the dimensionless parametric gap ratio γ_G, defined in the following equation, is introduced in the studies in this section.

$$\gamma_G = \frac{\Delta_G}{\Delta_{max}} \quad (4)$$

In the above equation, Δ_G is the spacing between the joints between the main and substructure, Δ_{max} is the minimum spacing between the joints to avoid collision between the main and substructure results under earthquake action. If $\gamma_G > 1$, no collision will occur between the two, and if $\gamma_G < 1$, a collision will occur. For the calculations in this section, $\gamma_G = 0.2$ was chosen to investigate the influence of collision on the structural response, and $\Delta_{max} = 300$ mm was defined.

The main factors affecting the collision of the main and sub-frames in a mega-sub isolated structure are the seismic intensity and direction, the spacing between the main and sub-frames, and the height of the sub-frames. The influences of changes in these parameters on the collision response of the main and sub-frames are analyzed below.

5.1.1. Collision Forces

After calculation, the collision force is simulated by the axial force in the linear elastic collision g_p unit, when the gap ratio $\gamma_G = 0.2$, the axial forces of the maximum collision unit under the action of the three seismic waves are shown in Table 2. Figure 10 depicts the time history diagram of the collision unit with maximum axial force.

Table 2. Peak collision forces between the main and substructure.

Seismic Wave	El Centro Wave	Taft Wave	Artificial Wave
Collision force/10^3 kN	58.89	48.77	41.93

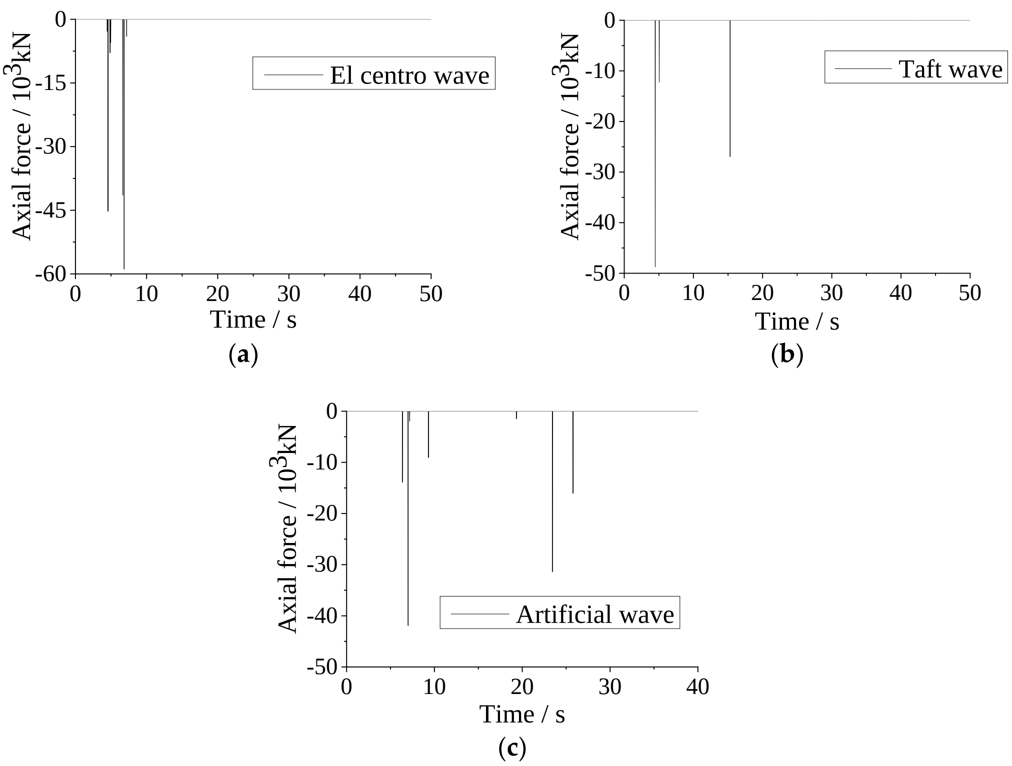

Figure 10. Time history diagram of collision unit with maximum axial force: (**a**) El Centro wave; (**b**) Taft wave; (**c**) Artificial wave.

Figure 10 above shows that the linear elastic collision units under the action of the three seismic waves, all occurred collisions between the main and subframes. Specifically, under the El Centro wave, there were 7 collisions, with a maximum collision force of 58.89×10^3 kN. Under the Taft wave, there were 3 collisions, with a maximum collision force of 48.77×10^3 kN. Under the artificial wave, there were 7 collisions, with a maximum collision force of 41.93×10^3 kN.

5.1.2. Acceleration

Figures 11 and 12 show the acceleration dynamic time curves of the third sub-frame and the top floor of the main frame for the collision and no-collision cases under the action of El Centro wave when the gap ratio γ_G = 0.2, respectively.

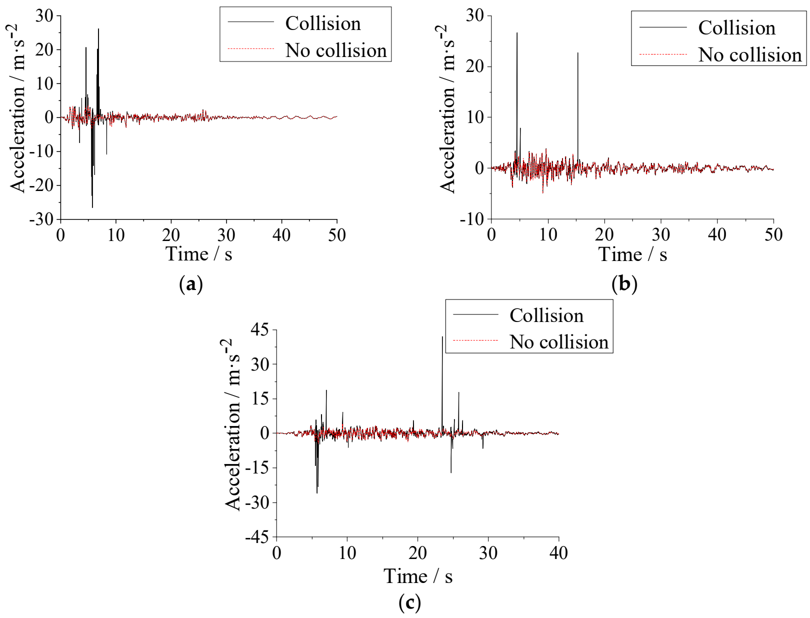

Figure 11. Comparison of acceleration time history for the third subframe: (**a**) El Centro wave; (**b**) Taft wave; (**c**) Artificial wave.

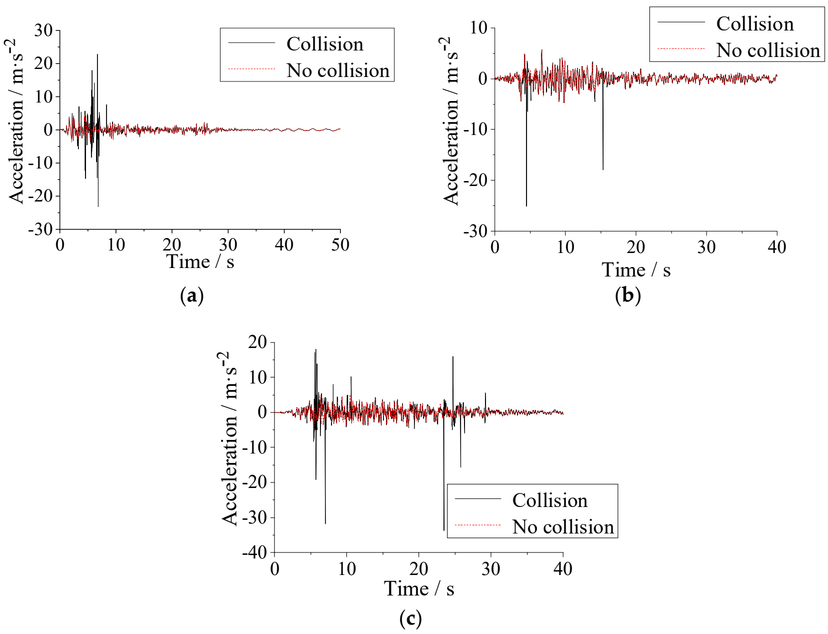

Figure 12. Comparison of acceleration time history at the top of the main frame: (**a**) El Centro wave; (**b**) Taft wave; (**c**) Artificial wave.

A comparison of the acceleration time curves shows that when the main and sub-frames collide, the peak acceleration of the sub-frame, as well as the main frame, increases to a large extent instantaneously, and the acceleration amplification of the main frame under collision is smaller than that of the sub-frame.

5.1.3. Base Shear

When the peak acceleration is 0.4 g and the gap ratio γ_G = 0.2, the time-history curves of the X-direction base shear force for the main frame under the action of El Centro wave, Taft wave, artificial wave, with and without collisions with the subframe, are shown in Figure 13.

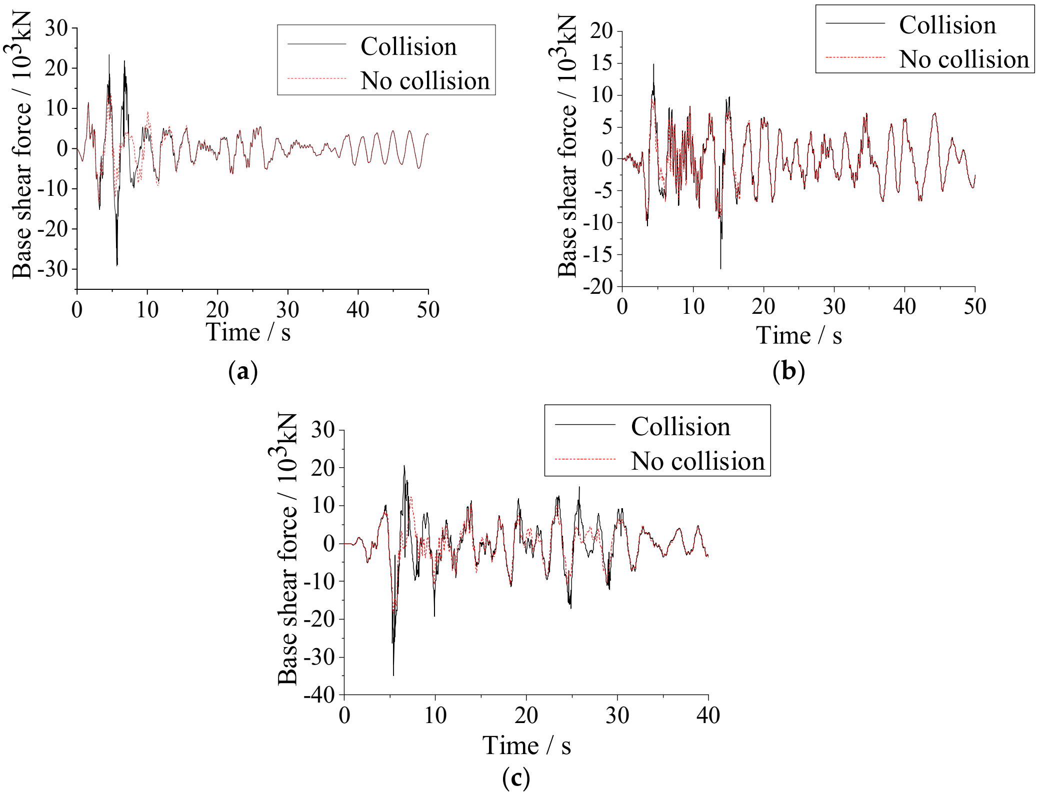

Figure 13. The time-history curves of the X-direction base shear force for the main frame: (**a**) El Centro wave; (**b**) Taft wave; (**c**) Artificial wave.

The time curve of the basal shear in the X-direction of the main frame of the mega-sub isolated structure shows that the main and subframes amplify the basal shear at the moment of collision and under the action of El Centro wave, Taft wave, and artificial wave, the base shear force was amplified by a factor of 2.11, 1.85, and 1.88, respectively. The impact of the collision on the structure is instantaneous and huge after the occurrence of the collision.

The results of the dynamic analysis after the collision of the main and sub-frame show that when the collision of the main and sub-frame occurs under the action of the earthquake, the linear elastic collision model g_p unit arranged between the seismic joints produces a huge instantaneous axial force, which is equivalent to applying a huge external force on top of the isolation sub-frame, making the peak acceleration of the sub-frame will also have a great amplification in an instant. The base sheer force of the structure will also be amplified instantly, which will greatly impact the safety and comfort of the main and sub-frame. It will have a greater influence on the safety and comfort of the main and subframes. Therefore, collisions between the main and subframes should be avoided as far as possible in practical engineering.

5.2. Influence of Ground Vibration Levels

In the model, the gap ratio γ_G = 0.2 is defined for the main and sub-frame, and only the peak acceleration is used as the variable, with El Centro wave, Taft wave, and artificial wave selected as input. The peak accelerations of the three seismic waves were amplitude modulated, and the peaks were amplified to five different levels of 0.3 g, 0.4 g, 0.5 g, 0.6 g, and 0.7 g, and then the structure was analyzed in time.

5.2.1. Base Shear

The simulated results of the time history analysis are shown in Tables 3–5, which shows that as the peak acceleration input increases, the collision force between the main and subframe and the number of collisions also change. As can be seen from Figures 14 and 15, the increase in peak collision force and the peak acceleration under collision (the analysis of the influence of acceleration below refers to the acceleration of the third subframe under collision of the main and substructure) are not positively correlated, as the acceleration peak increases the collision force will appear to decrease, but as the peak acceleration increases, the collision frequency will also increase.

Table 3. Influence of El Centro waves on collision forces.

Earthquake Peak/g	0.3	0.4	0.5	0.6	0.7
Peak collision force/10^3 kN	36.55	58.89	57.44	77.5	62.45
Number of collisions	5	7	5	13	15

Table 4. Influence of Taft wave on collision forces.

Earthquake Peak/g	0.3	0.4	0.5	0.6	0.7
Peak collision force/10^3 kN	6.96	48.77	43.88	46.14	91.50
Number of collisions	1	3	5	13	19

Table 5. Influence of artificial wave on collision forces.

Earthquake Peak/g	0.3	0.4	0.5	0.6	0.7
Peak collision force/10^3 kN	62.16	41.93	89.37	64.87	95.52
Number of collisions	2	7	15	27	41

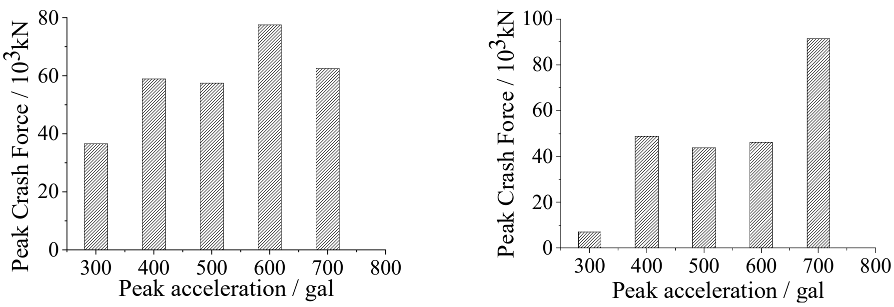

(**a**) (**b**)

Figure 14. *Cont.*

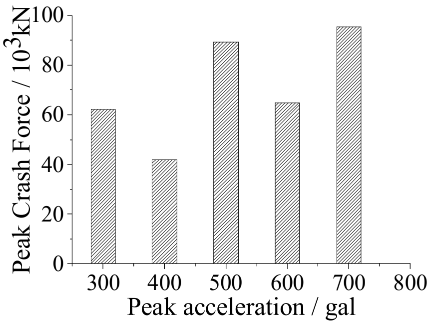

(**c**)

Figure 14. Variation of peak collision force between the mainframe and sub-frame with peak acceleration under different seismic waves: (**a**) El Centro wave; (**b**) Taft wave; (**c**) Artificial wave.

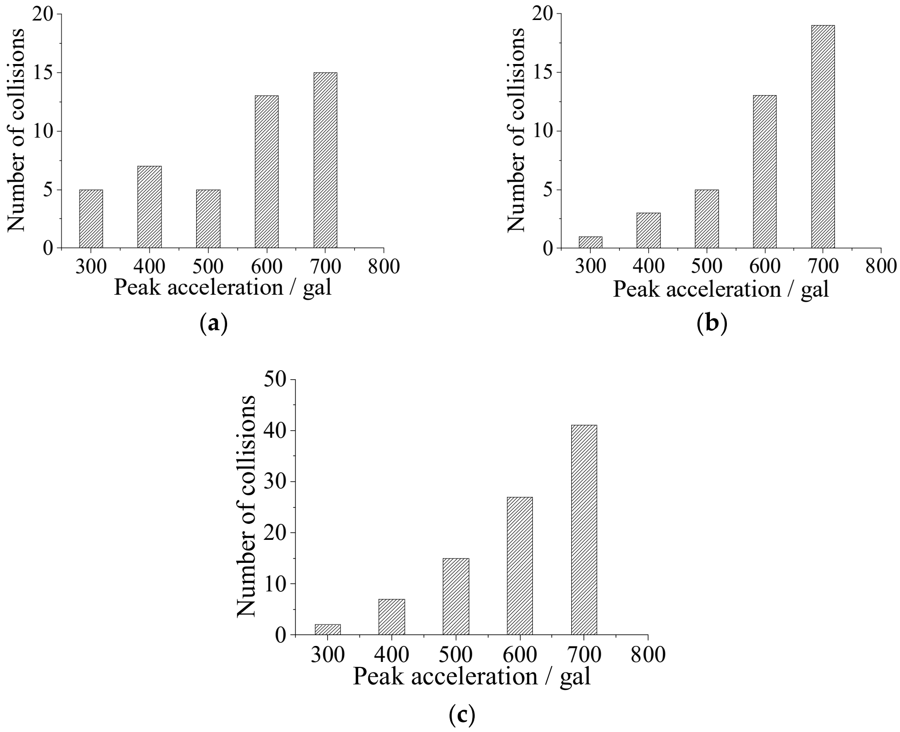

Figure 15. Variation of the number of main and subframe collisions with peak seismic acceleration under different seismic waves: (**a**) El Centro wave; (**b**) Taft wave; (**c**) Artificial wave.

5.2.2. Influence on Acceleration

The peak acceleration of the top layer of the third sub-frame is shown in Table 6, and it can be seen that the peak acceleration of the sub-frame is larger under collision. It can be seen from Figure 16 that the peak variation pattern of acceleration is relatively consistent, and they all increase with the increase of the peak seismic wave. The acceleration is inconsistent with the change of collision force, and the acceleration value is not necessarily the largest when the collision force is the largest and there is no direct connection between the two.

Table 6. Influence of seismic waves on collision acceleration.

Earthquake Peak/g	0.3	0.4	0.5	0.6	0.7
El Centro wave/m·s^{-2}	26.52	26.57	80.93	100.08	108.8
Taft wave/m·s^{-2}	22.87	26.65	71.13	86.51	102.5
Artificial wave/m·s^{-2}	26.60	42.01	83.23	99.01	119.5

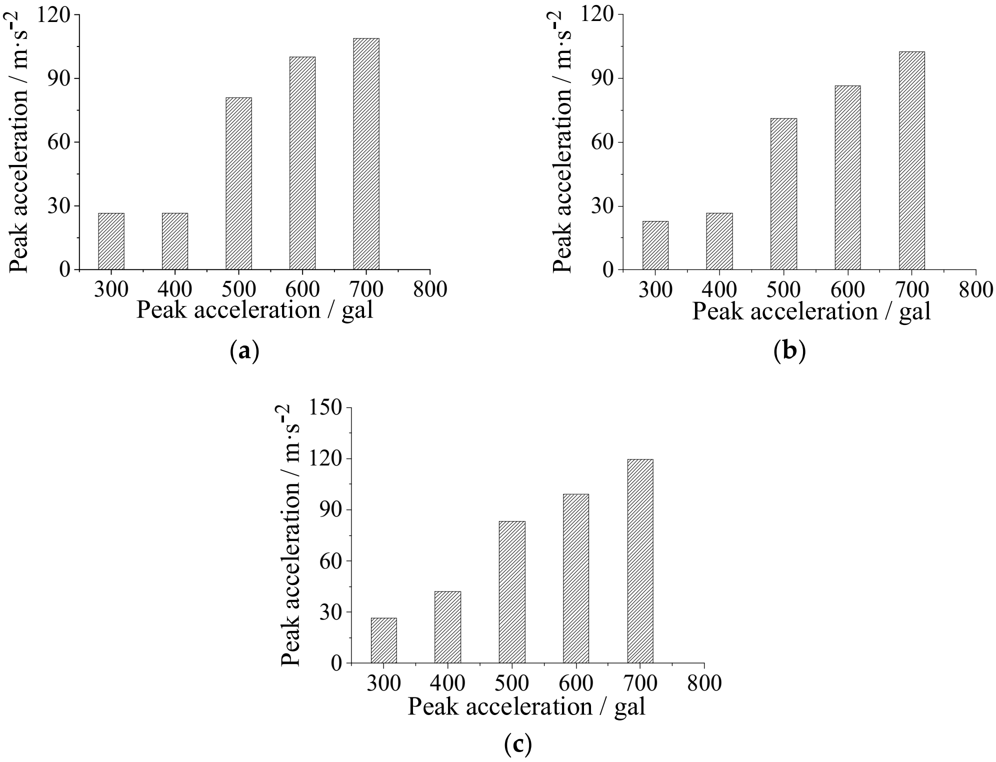

Figure 16. The influence of seismic acceleration variation on the top floor acceleration of the third subframe: (**a**) El Centro wave; (**b**) Taft wave; (**c**) Artificial wave.

5.3. Influence of Main and Substructure Spacing

The spacing between the main and sub-frames in the mega-sub isolated structure is an important factor that directly affects whether the two collide. In this section, the gap ratio γ_G of the main and sub-structures is taken as the independent variable, and the influence of the distance between the main and sub-frames on the collision is studied by changing the value of γ_G.

5.3.1. Influence on Collision Forces

Table 7 shows the change of the peak collision force of the main and subframe with the gap ratio, from which it can be seen that the change of the collision force is more obvious with the increase of the spacing between the two. The peak collision forces vary significantly under the influences of different seismic waves. Specifically, the peak collision force under the El Centro wave is 66.74×10^3 kN. Under the Taft wave, it is 49.13×10^3 KN. Under the artificial wave, it is 51.88×10^3 kN. From the shown in Figure 17, it can be seen that the collision force does not decrease with the increase of the spacing between the main and subframe, and the peak collision force does not appear when the spacing is minimum.

Table 7. Influence of gap ratio on collision forces.

Gap Ratio	0.1	0.2	0.3	0.4	0.5	0.6	0.7
El Centro	47.76	58.89	39.12	26.87	51.39	56.17	66.74
Taft wave	37.23	48.77	12.05	28.46	49.13	23.26	17.11
Artificial wave	51.88	41.93	33.40	27.74	48.98	41.34	24.21

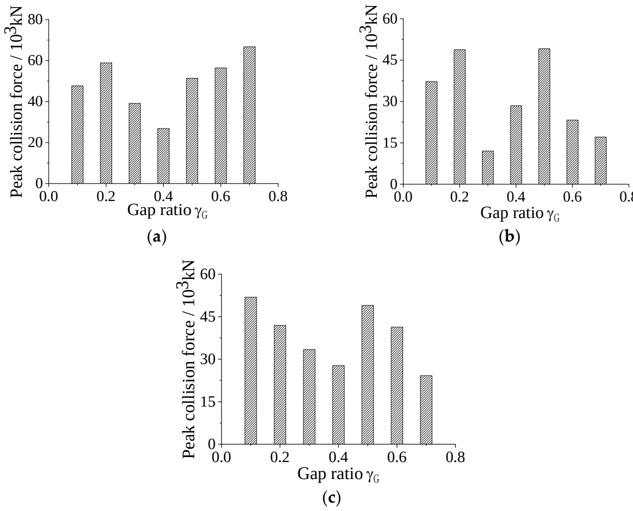

Figure 17. Variation of peak collision force between the main frame and sub-frame with gap ratio under different seismic waves: (**a**) El Centro wave; (**b**) Taft wave; (**c**) Artificial wave.

5.3.2. Influence on Acceleration

The response values of collision acceleration in Table 8 show that the main and sub-frame spacing has a greater influence on the acceleration peak under sub-frame collision. It can be seen from Figure 18 that under the action of the three seismic waves, the variation pattern of the peak collision acceleration response of the third subframe with the increase in gap ratio is similar. Generally, it shows a decreasing trend, followed by an increase and then another decrease. However, the moment where the peak acceleration values occur differs under the influences of different earthquake motions. It indicates that specific analysis should be conducted based on the adopted seismic waves when studying and analyzing collision issues.

Table 8. Influence of gap ratio on third sub-frame collision acceleration.

Gap Ratio	0.1	0.2	0.3	0.4	0.5	0.6	0.7
El Centro	65.0	26.57	37.84	62.47	88.07	108.1	69.03
Taft wave	39.81	26.65	47.27	56.62	37.44	20.54	16.17
Artificial wave	77.32	42.01	90.4	42.65	57.89	69.63	41.32

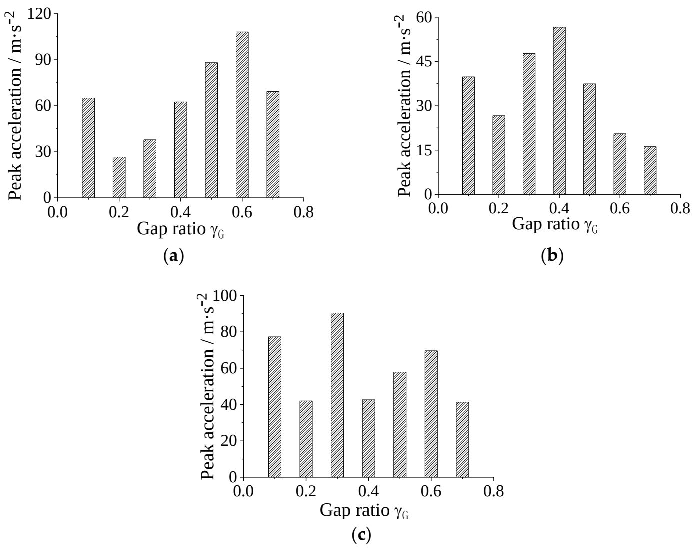

Figure 18. The influence of gap ratio variation on the top floor acceleration of the third subframe under different seismic waves: (**a**) El Centro wave; (**b**) Taft wave; (**c**) Artificial wave.

5.4. Influences of Vertical Earthquakes

Due to the lower vertical stiffness of the mega sub-structure, the dynamic response of both the main and substructures will be greater when considering the vertical seismic action compared to the response under unidirectional horizontal seismic action. In this section, the dynamic response of the giant structure under different excitation modes (X-direction, X + Z-direction) will be analyzed using El Centro wave, Taft wave, and artificial wave in sequence. The peak acceleration of the earthquake is set to 0.4 g, and the gap ratio γ_G is set to 0.2. The study considers the dynamic response of the main and substructures when subjected to vertical seismic action.

5.4.1. Influence on Collision Forces

The peak collision force under coupled directional ground shaking will be larger than that under unidirectional excitation, consistent with the acceleration response law. The involvement of the vertical earthquake component will also amplify the collision force by a factor of about 15%. As can be seen from Figure 19, under coupled earthquake excitation, the peak collision force of the main and sub-frame will not only increase, but the first collision will also occur slightly earlier than under one-way excitation, and the number of collisions will also be slightly more than under one-way excitation. The specific values can be found in Table 9.

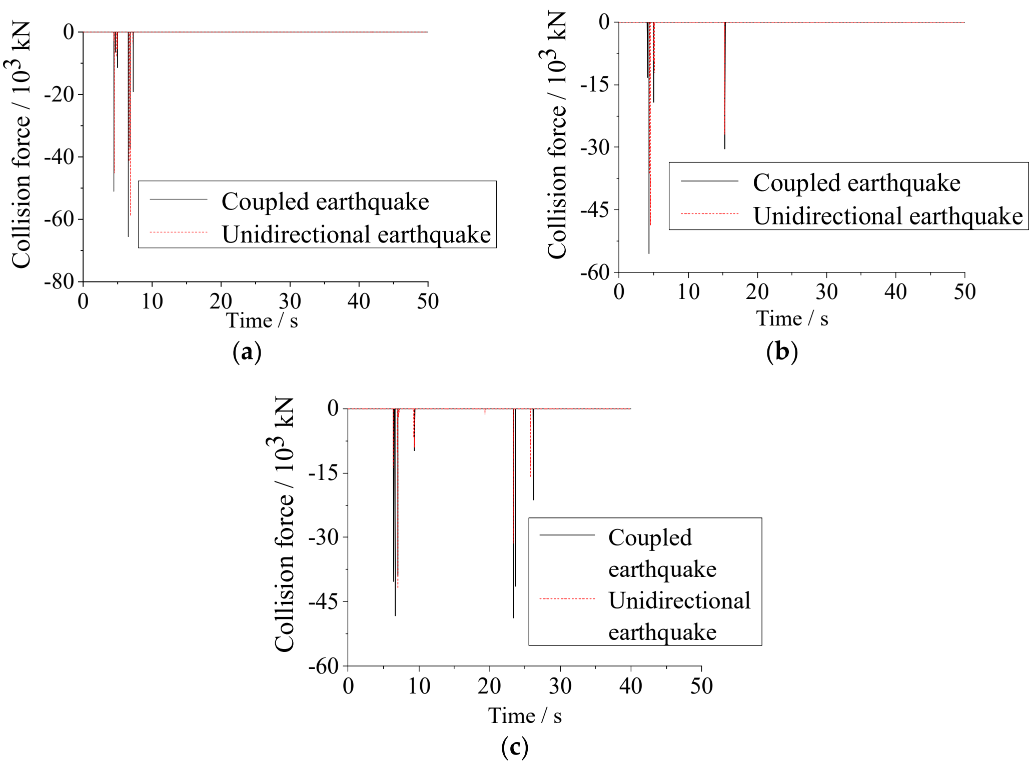

Figure 19. The collision force time history curves of the main and substructures under different seismic waves: (**a**) El Centro wave; (**b**) Taft wave; (**c**) Artificial wave.

Table 9. The peak collision forces under three types of excitations.

Seismic Wave	Unidirectional Excitation	Coupled Excitation	Amplification Factor
El Centro	58.89	65.57	11.3%
Taft wave	48.77	55.50	13.8%
Artificial wave	41.93	48.35	15.3%

5.4.2. Influence on Acceleration

When vertical earthquake influences are considered, the peak acceleration under subframe collision is greater than the acceleration value under unidirectional excitation, with an amplification of around 20%, indicating that the involvement of vertical earthquake amplifies the collision influence of the main and substructure. The comparison of the time curves in Figure 20 shows that the collision is instantaneous and only influences a certain instant. The collision acceleration response varies significantly for different seismic waves. It can be seen that there is an amplification of the post-collision acceleration due to the small vertical stiffness of the isolated bearing. The specific values can be found in Table 10.

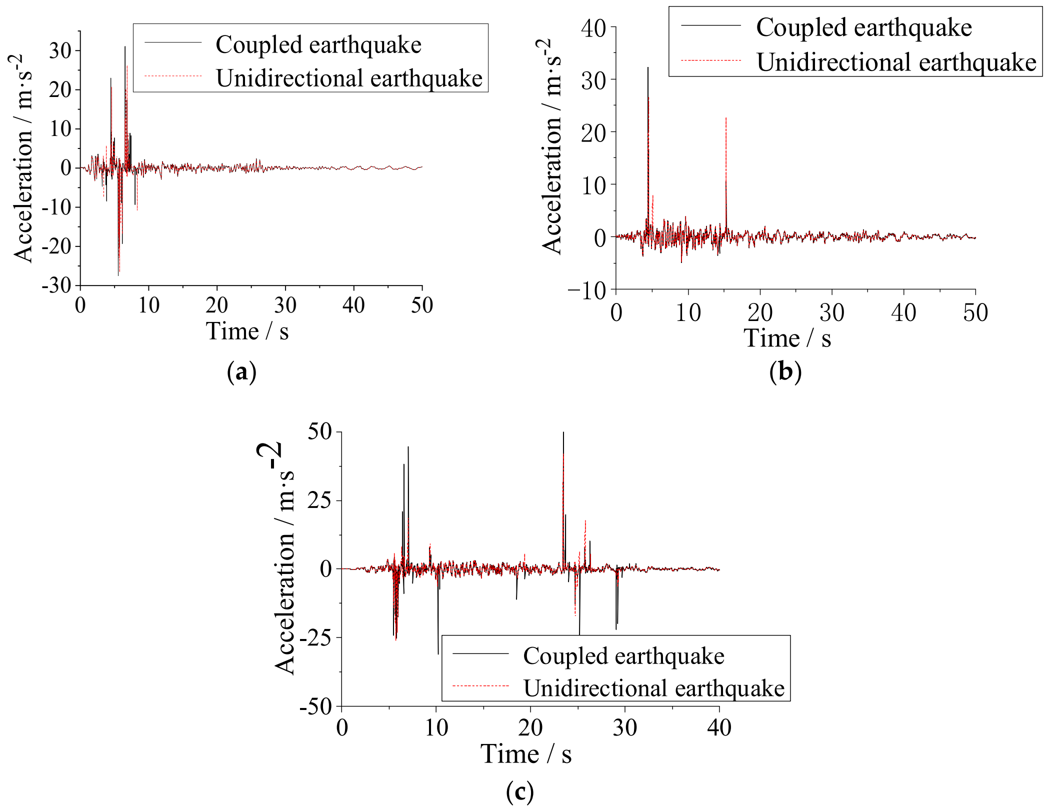

Figure 20. Time history curve of collision acceleration for the third subframe under different seismic waves: (**a**) El Centro wave; (**b**) Taft wave; (**c**) Artificial wave.

Table 10. Peak collision acceleration of the third subframe under different excitation methods and seismic waves.

Seismic Wave	Unidirectional Excitation	Coupled Excitation	Amplification Factor
El Centro	26.57	31.09	17.01%
Taft wave	26.65	32.26	21.05%
Artificial wave	42.01	49.95	18.90%

5.5. Influence of Subframe Height

In order to study the influence of the seismic isolation subframe on the collision response of main and subframes, this subsection changes the height of the subframe by increasing the number of layers of the subframe based on the original mega-sub isolated structure model. It establishes a main frame structure that can accommodate 12 layers of subframes, and the step size of the subframe increase is 1 layer. In order to facilitate the study, the gap ratio γ_G between the main frame and subframe is kept constant at 0.2, and the rest of the parameters are kept unchanged. Similarly, we have selected three seismic waves, namely El Centro wave, Taft wave, and artificial wave, for collision research, and the peak earthquake acceleration amplitude of 0.4 g.

5.5.1. Influence on Collision Forces

Figure 21 shows the change of the peak collision force of the main and substructure with the change of substructure height under the action of three seismic waves earthquakes. It can be seen that the changing pattern of the peak collision force under the action of three seismic waves is quite different. Under the action of the El Centro wave, the peak collision force exhibits a trend of initially decreasing, then increasing, followed by another decrease, and finally continuing to increase. The maximum collision force occurs when the substructure has 6 stories. For the Taft wave, the peak collision force generally follows a trend of initially decreasing, then increasing, and then decreasing again. The maximum peak collision force occurs when the total number of substructure stories is 10. As for the artificial wave, the variation pattern of the peak collision force is similar to that of the El Centro wave. The maximum collision force occurs when the total number of substructure stories is 12.

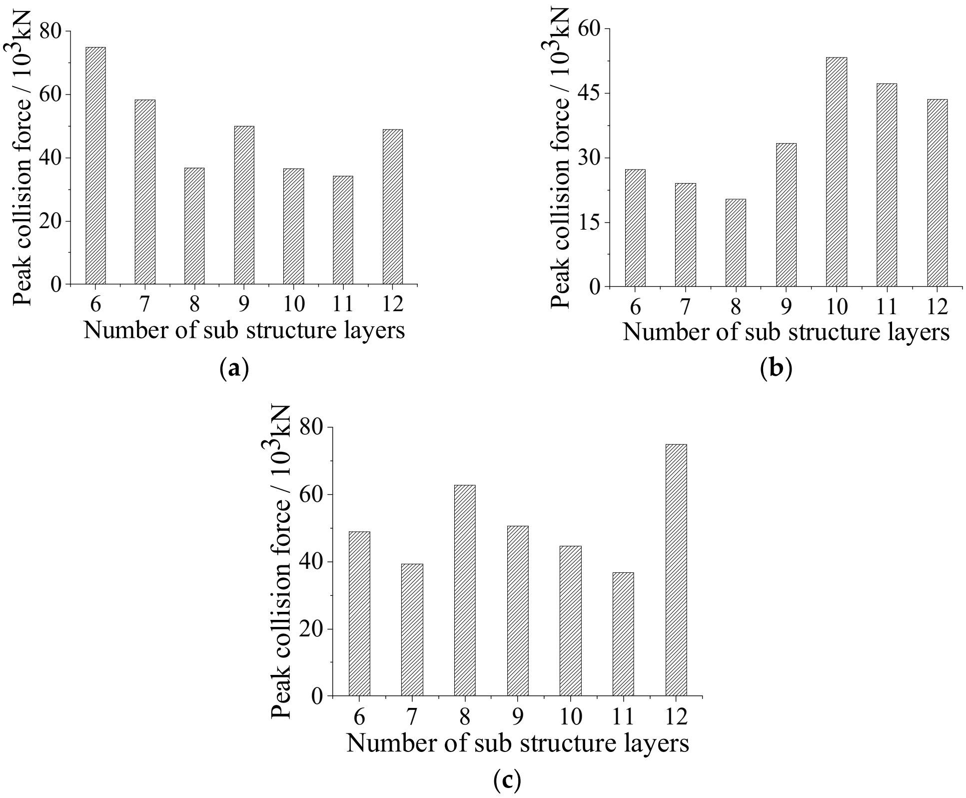

Figure 21. Influence of substructure height variation on the peak collision force in the main and substructures at different seismic waves: (**a**) El Centro wave; (**b**) Taft wave; (**c**) Artificial wave.

For the sub-structure, the impact of its height on the main and sub-structure under different earthquake actions need to be more consistent. Therefore, when designing the height of the sub-structure, specific analysis, and reasonable design should be carried out according to different load conditions.

5.5.2. Influence on Acceleration

Figure 22 shows the variation of the peak acceleration with a height of the substructure under the collision of the main and substructure. The figure below shows that the acceleration variation pattern is more related to the form of the input ground shaking. The acceleration value under the action of the El Centro wave decreases, then increases and decreases, when the collision acceleration between the main and substructures is maximum, and the total number of substructure stories is 6. Under the action of the Taft wave, the acceleration shows a trend of decreasing, increasing, and decreasing, When the collision acceleration between the main and substructures is maximum, the total number of substructure stories is 12. Under the action of the artificial wave, the acceleration first increases, and then decreases, When the collision acceleration between the main and substructures is maximum, the total number of substructure stories is 8.

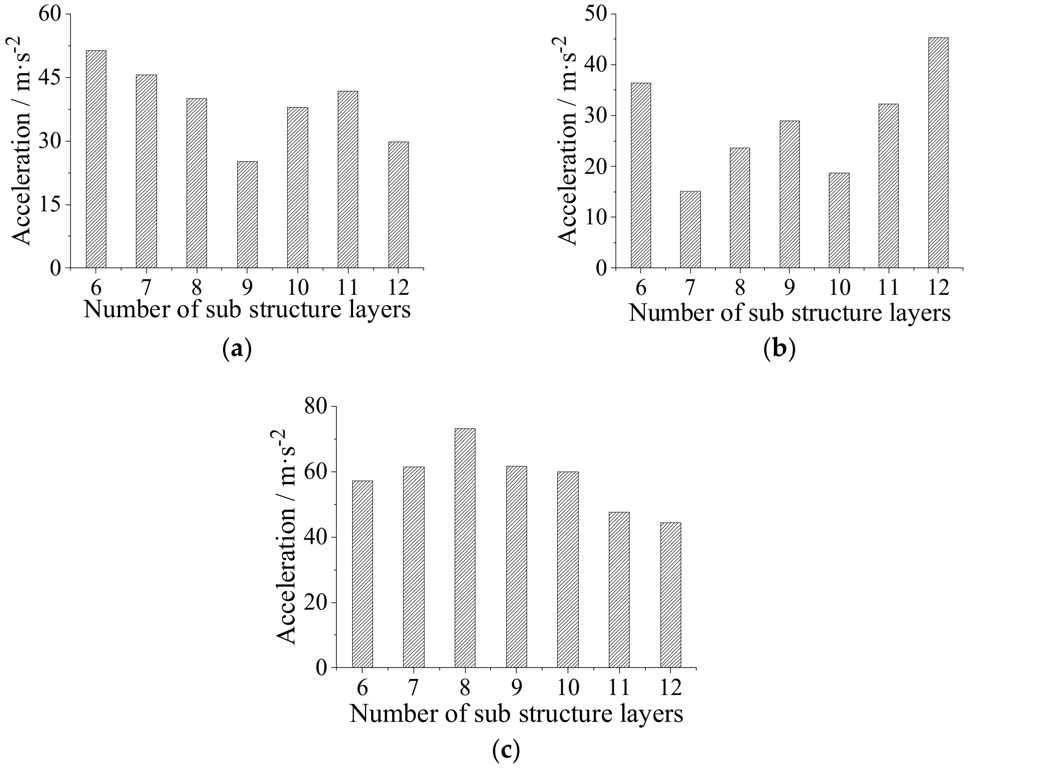

Figure 22. Influence of substructure height variation on the peak collision acceleration force in the main and substructures at different seismic waves: (**a**) El Centro wave; (**b**) Taft wave; (**c**) Artificial wave.

It can be seen that the change in acceleration and collision force is not positively correlated with the change in layer height, and there is no necessary connection between the two. The response law is more related to the type of seismic wave, so when considering the influence of layer height on collision, a specific analysis should be carried out according to different layers and seismic waves.

6. Conclusions

This paper analyzed the dynamic response of the mega sub-isolated structure under horizontal and coupled earthquakes. In addition, the collision of the main and sub-frames of the mega-sub isolated structure was simulated, and the parameters that affect the collision response were studied. The following conclusions were drawn:

(a) The study found that changes in the damping ratio, mass ratio, and frequency ratio will influence the displacement and acceleration peaks of the dynamic response of the main and sub-frames. In this paper, the optimal parameter values of each item are obtained through numerical method research. The horizontal isolation effect is the best when the horizontal damping ratio is 0.3, the horizontal frequency ratio is 0.6, and the mass ratio is 3.0, while the vertical damping ratio of 0.2 and the vertical frequency ratio of 1.2 have the best effect on isolation, thus the parameters need to be set according to the actual requirements during engineering design.

(b) Through collision simulation, it is found that instantaneous and huge collision force will be generated when the main structure and the sub-structure collide, and the response value of acceleration and base shear force will be amplified instantaneously. It will have a significant impact on the safety and comfort of the structure. The amplification factor of peak acceleration of the main structure is smaller than that of the sub-structure, and the peak value of collision force is not positively correlated with the peak value of acceleration. With the increase of peak acceleration, the collision force curve will appear decline section. Similarly, the peak value of the collision force does not decrease with the increase in the distance between the main structure and the substructure. The peak value of the collision force is not at the minimum distance, but the increase in the peak collision force will also lead to an increase in the occurrence frequency of collisions between the main and substructure.

(c) Under the excitation of coupled earthquakes, the vertical earthquake component will amplify the collision response between the main structure and the substructure and slightly advance the collision occurrence time. Furthermore, under the one-way excitation, the acceleration after the collision will be amplified due to the small stiffness of the isolation bearing. In addition, the change in acceleration and collision force is not positively correlated with the change in story height, and there is no necessary connection between the two. When considering the impact of story height on collision, it is necessary to conduct a specific analysis according to the number of floors and wave type. Under different earthquake actions, the dynamic response patterns of the mega substructure isolated structure vary. Therefore, it is important to consider and compare various aspects during the structural design process to select the optimal parameters.

Through the above conclusions, we can know the optimal parameter values of the mega sub-isolated structure under multiaxial earthquakes and, at the same time, understand the dynamic response of the structure in the case of collision and the influence of related parameters on it, which provides a basis for further optimization of the mega sub isolated structure and practical application in engineering.

Author Contributions: Data curation, H.M.; Formal analysis, W.L.; Investigation, W.L. and G.L.; Project administration, X.Y.; Resources, X.Y.; Supervision, X.Y.; Writing—original draft, G.L.; Writing—review and editing, W.L. and J.L. All authors have read and agreed to the published version of the manuscript.

Funding: This work was financially sponsored by National Natural Science Foundation of China [Grant NO. 52278490], the Science and Technology Planning Project of Fujian [Grant NO. 2022Y3001, 2023J01343] and the Science and Technology Planning Project of Fuzhou [Grant NO. 2021-Y-082].

Institutional Review Board Statement: Not applicable.

Informed Consent Statement: Not applicable.

Data Availability Statement: Not applicable.

Conflicts of Interest: The authors declare no conflict of interest.

References

1. Szolomicki, J.; Golasz-Szolomicka, H. Technological advances and trends in modern high-rise buildings. *Buildings* **2019**, *9*, 193. [CrossRef]
2. Elias, S.; Matsagar, V. Research developments in vibration control of structures using passive tuned mass dampers. *Annu. Rev. Control* **2017**, *44*, 129–156.
3. Briman, V.; Ribakov, Y. Using seismic isolation columns for retrofitting buildings with soft stories. *Struct. Des. Tall Spec. Build.* **2009**, *18*, 507–523. [CrossRef]
4. De Domenico, D.; Ricciardi, G. Earthquake-resilient design of base isolated buildings with TMD at basement: Application to a case study. *Soil Dyn. Earthq. Eng.* **2018**, *113*, 503–521.
5. Ribakov, Y. Base-isolated structures with selective controlled semi-active friction dampers. *Struct. Des. Tall. Spec. Build.* **2011**, *20*, 757–766. [CrossRef]

6. Yun, Z.; Lu, X.L. Analysis of factors influencing dynamic characteristics of mega-structure. *J. Eng. Mech.* **2008**, *25*, 53–56. (In Chinese)
7. Kim, H.S.; Kang, J.W. An efficient structural analysis of super tall mega frame buildings using a multi-level condensation method. *J. Asian Archit. Build. Eng.* **2012**, *11*, 343–350. [CrossRef]
8. Feng, M.Q.; Mita, A. Vibration control of tall buildings using mega subconfiguration. *J. Eng. Mech.* **1995**, *121*, 1082–1088. [CrossRef]
9. Chai, W.; Feng, M.Q. Vibration control of super tall buildings subjected to wind loads. *Int. J. Nonlinear Mech.* **1997**, *32*, 657–668. [CrossRef]
10. Mita, A.; Kaneko, M. Mega-Sub Control System for Reducing Seismic Response of Tall Buildings. In *Post-Earthquake Rehabilitation and Reconstruction*; Pergamon: Oxford, UK, 1996; pp. 309–315.
11. Sadek, F.; Mohraz, B.; Taylor, A.W.; Chung, R.M. A method of estimating the parameters of tuned mass dampers for seismic applications. *Earthq. Eng. Struct. D* **1997**, *26*, 617–635. [CrossRef]
12. Wei, Z.; Ye, J.J. Research of Earthquake Resistance Performance on the Mega-Sub Controlled Structure. *Appl. Mech. Mater.* **2013**, *353*, 2196–2201. [CrossRef]
13. Limazie, T.; Zhang, X.A.; Wang, X. Vibration control parameters investigation of the mega-sub controlled structure system (MSCSS). *Earthq. Struct.* **2013**, *5*, 225–237. [CrossRef]
14. Abdulhadi, M.; Xun'an, Z.; Fan, B.; Moman, M. Design, optimization and nonlinear response control analysis of the mega sub-controlled structural system (MSCSS) under earthquake action. *J. Earthq. Tsunami* **2020**, *14*, 2050013. [CrossRef]
15. Shahzad, M.M.; Zhang, X.A.; Wang, X.; Abdulhadi, M.; Wang, T.; Xiao, Y. Response control analysis of a new mega-sub controlled structural system (MSCSS) under seismic excitation. *Struct. Des. Tall. Spec. Build.* **2022**, *31*, e1935. [CrossRef]
16. Ziyaeifar, M.; Noguchi, H. Partial mass isolation in tall buildings. *Earthq. Eng. Struct. D* **1998**, *27*, 49–65. [CrossRef]
17. De Silva, C.W. (Ed.) *Vibration and Shock Handbook*; CRC Press: Boca Raton, FL, USA, 2005.
18. Lan, Z.; Tian, Y.; Fang, L.; Liang, S.; Wang, X. An experimental study on seismic responses of multifunctional vibration-absorption reinforced concrete megaframe structures. *Earthq. Eng. Struct. D* **2004**, *33*, 1–14. [CrossRef]
19. Shu, G.P.; Zhang, Y.F.; Lu, Z.T.; Zuo, J.; Xia, C.C.; Jiang, H. The aseismic capability and shaking table experiment of mega-frame structures. *Innov. Sustain. Struct.* **2005**, *1*, 398–414.
20. Li, X.; Tan, P.; Li, X.; Liu, A. Mechanism analysis and parameter optimization of mega-sub-isolation system. *Shock Vib.* **2016**, *5*, 2605839. [CrossRef]
21. Tan, P.; Zhang, Y.; Li, X.; Liu, A.; Zhou, F. Experimental investigation of mega-sub isolation structure. *Struc.t Des. Tall. Spec. Build.* **2017**, *26*, e1360. [CrossRef]
22. Anajafi, H.; Medina, R.A. Comparison of the seismic performance of a partial mass isolation technique with conventional TMD and base-isolation systems under broad-band and narrow-band excitations. *Eng. Struct.* **2018**, *158*, 110–123. [CrossRef]
23. Kim, S.J. *Seismic Assessment of RC Structures Considering Vertical Ground Motion*; UIUC: Champaign, IL, USA, 2008.
24. Shingu, K.; Fukushima, K. Seismic isolation and fuzzy vibration control of shell structure subjected to vertical seismic forces. *Jpn. Soc. Mech. Eng.* **1994**, *60*, 2999–3005.
25. Chung, W.J.; Yun, C.B.; Kim, N.S.; Seo, J.W. Shaking table and pseudodynamic tests for the evaluation of the seismic performance of base-isolated structures. *Eng. Struct.* **1999**, *21*, 365–379. [CrossRef]
26. Han, J.P.; Zhou, W. Preliminary analysis of vertical ground motion characteristics of Wenchuan earthquake. *J. Eng. Mech.* **2012**, *29*, 211–219. (In Chinese)
27. Furukawa, S.; Sato, E.; Shi, Y.; Becker, T.; Nakashima, M. Full-scale shaking table test of a base-isolated medical facility subjected to vertical motions. *Earthq. Eng. Struct. D* **2013**, *42*, 1931–1949. [CrossRef]
28. Guzman Pujols, J.C.; Ryan, K.L. Computational simulation of slab vibration and horizontal-vertical coupling in a full-scale test bed subjected to 3D shaking at E-Defense. *Earthq. Eng. Struct. D* **2018**, *47*, 438–459. [CrossRef]
29. Yan, X.Y.; Qi, A.; Mao, H.M. Multi-dimensional seismic response analysis of three-dimensional seismic-isolation mega-sub structure. *Chin. Civ. Eng. J.* **2017**, *50*, 36–46. (In Chinese)
30. De Domenico, D.; Losanno, D.; Vaiana, N. Experimental tests and numerical modeling of full-scale unbonded fiber reinforced elastomeric isolators (UFREIs) under bidirectional excitation. *Eng. Struct.* **2023**, *274*, 115118. [CrossRef]
31. Scislo, L. High activity earthquake swarm event monitoring and impact analysis on underground high energy physics research facilities. *Energies* **2022**, *15*, 3705.
32. Tian, Y.J. *Damping Principle and Optimization Design Method of Multifunctional Damping Structure of Mega Frame*; Southeast University: Nanjing, China, 2002. (In Chinese)
33. Lan, Z.J.; Tian, Y.J.; Cao, S.Y.; Wang, H.H. Analysis of vibration damping mechanism and damping effect of multifunctional vibration-damping structural system with mega frame. *Chin. Civ. Eng. J.* **2002**, *35*, 1–5. (In Chinese)
34. Sheng, Z.H.; Chen, H. Seismic analysis of giant frame structures. *Ind. Constr.* **2006**, *51*, 192–194+252. (In Chinese)
35. Xin, C.L. Seismic response time analysis method. *Technol. Econ. Areas Commun.* **2010**, *12*, 50–53. (In Chinese)
36. Zhou, Y.Z.; Zhou, Y. Design of High Damping HNBR Isolation Bearings for Bridges. *Rub. Plast. Technol. Equip.* **2021**, *47*, 36–40. (In Chinese)
37. Li, Y.; Zong, Z.; Huang, X.; Xia, J.; Li, L. Experimental study on mechanical properties of high damping rubber bearing model. *IOP Conf. Ser. Earth Environ. Sci.* **2017**, *61*, 012105. [CrossRef]

38. Falborski, T.; Jankowski, R. Experimental study on effectiveness of a prototype seismic isolation system made of polymeric bearings. *Appl. Sci.* **2017**, *7*, 808. [CrossRef]
39. Pourmasoud, M.M.; Lim, J.B.P.; Hajirasouliha, I.; McCrum, D. Multi-directional base isolation system for coupled horizontal and vertical seismic excitations. *J. Earthq. Eng.* **2022**, *26*, 1145–1170. [CrossRef]